Z-spectral modeling for CEST-MRI of bladder cancer

Ryan Nicholas Schurr[1], Huyen T. Nguyen[2], Kamal Pohar[3], Amir Mortazavi[4], Zarine Shah[2], Debra Zynger[5], Michael V. Knopp[2], and Guang Jia[1]

[1]Department of Physics and Astronomy, Louisiana State University, Baton Rouge, Louisiana, United States, [2]Department of Radiology, The Ohio State University, Ohio, United States, [3]Department of Urology, The Ohio State University, Ohio, United States, [4]Department of Internal Medicine, The Ohio State University, Ohio, United States, [5]Department of Pathology, The Ohio State University, Ohio, United States

Introduction

In 2014 there are expected to be 74,690 new cases of bladder cancer and 15,580 related deaths, accounting for over 4% of all cancer incidences and approximately 3% of all cancer deaths.[1] Chemical exchange saturation transfer (CEST) MRI experiments produce contrast based on exchange of bulk water protons with saturated solute protons. CEST-MR imaging is quantified by the asymmetry of the magnetization transfer ratio, $MTR_{asym}(\omega) = MTR(-\omega) - MTR(\omega)$.[2] Z-spectra are shifted using a B_0 map to correct for B_0 inhomogeneity, and the adjusted spectra are often fit with high order polynomial functions to calculate an adjusted adjusted MTR_{asym} value.[3] The effect seen in CEST-MR imaging of proteins occurs downfield from water at 3.5 ppm and 2.0 ppm frequency offsets,[4] so the portion of the Z-spectrum upfield from water may be described by a two-pool exchange model for magnetization transfer (MT) between the bulk water pool and a bound pool of protons associated with immobile macromolecules.[5] This study is to distinguish bladder cancer from normal bladder wall by separating the Z-spectra into upfield and downfield components and fitting these components separately.

Materials and methods

Subjects A total of 16 bladder cancer patients (13 male, 3 female, average age 69.5 years) were evaluated with MRI prior to radical cystectomy. The stage of disease ranged from pT1 to pT4a, with eight of the patients having disease staged T3a or higher.

MRI Patients were imaged on a 3.0 T MR system (Philips Achieva, Best, Netherlands) using a 32-channel phased array coil using a single-shot, single-slice turbo spin echo sequence (ssTSE) with a TR/TE of 6100 ms/56 ms, flip angle 90˚, field of view 140 × 140 mm^2, acquisition matrix 80 × 65, and slice thickness 6 mm. A radiofrequency (RF) saturation pre-pulse was applied prior to image acquisition consisting of sixteen 1800˚ block pulses with pulse lengths of 29-31 ms. A total of 33 images were acquired with the prepulse applied at varying frequency offsets ranging from 8 to -8 ppm in 0.5 ppm increments. Additionally, one image was acquired in the absence of saturation for signal normalization, and a B_0 map was acquired to apply a B_0 inhomogeneity correction during image analysis. The total acquisition time was 3.5 minutes.

Image Analysis Regions of interest (ROIs) were delineated for NBW and tumor based on pathology reports and T2-weighted images. Z-spectral data were acquired from each region using in-house software based on the Interactive Data Language (IDL, Exelis Visual Information Solutions, Boulder, CO). The data was separated into upfield and downfield components and fit using a non-linear least squares curve fitting package in IDL version 8.2. The data downfield from water were fit to an 8th order polynomial function, while the data upfield from water were fit to the function described by equation 1. MTR_{asym} values at 3.5 ppm and 2.0 ppm frequency offsets were calculated for each ROI by evaluating MTR(-ω) using the two-pool fit and MTR(+ω) using the 8th order polynomial fit.

$$\frac{S(\Delta\omega)}{S_0} = 1 - \frac{A_w\left(\frac{G_w}{2}\right)^2}{\left(\frac{G_w}{2}\right)^2 + \Delta\omega^2} - A_b \exp\left[-\left(\frac{1}{2}\right)\left(\frac{\Delta\omega}{390}\right)^2\right] \quad \text{(Equation 1)}^5$$

Where A_w and G_w are the magnitude and full width at half maximum of the Lorentzian function describing direct saturation of the bulk water pool (DWS), A_b is the magnitude of the broad Gaussian function describing MT with immobile macromolecules, $S(\Delta\omega)$ is the signal acquired with the saturation pulse applied at an offset frequency $\Delta\omega$, and S_0 is the signal without saturation.

Statistical Analysis A two-tailed, paired student's *t*-test was used to test for significant differences in A_w, G_w, A_b, and MTR_{asym} values between the NBW and tumor regions for all patients.

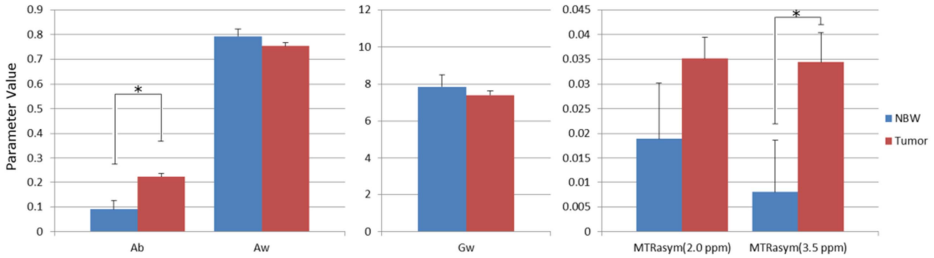

Figure 1: Average values for each fitting parameter and calculated MTR asymmetry values. A * denotes a significant difference between values in the NBW and tumor regions. Error bars represent one standard error of the mean.

Results and Discussion

Average values for all parameters and MTRasym values between the NBW and tumor regions are shown in Figure 1. Pairwise statistically significant differences between the tumor and NBW regions were found for A_b and MTR_{asym}(3.5 ppm) (*p*-values 0.003 and 0.03, respectively). There were no statistically significant differences between the tumor and NBW regions for A_w, G_w, or MTR_{asym}(2.0 ppm). A_b is analogous to the MTR values at larger frequency offsets that are obtained from MT experiments involving transfer of magnetization from immobile macromolecules.[6] The significant differences for A_b and MTR_{asym}(3.5 ppm) imply that these quantities have the potential to distinguish between NBW and bladder cancer.

Conclusion

Separately modeling the components of the Z-spectrum upfield and downfield from water can be applied in CEST-MRI experiments to distinguish bladder cancer from NBW using MTR_{asym}(3.5 ppm) values. This method provides information equivalent to MTR values from classic MT-MRI experiments through the parameter A_b, which may also have the ability to differentiate bladder cancer from NBW.

References

[**1**] Siegel R, et al. CA Cancer J. Clin. 2014; 64(1):9-29, [**2**] Zhou J, et al. Appl. Magn. Reson. 2012; 42(3):393-402, [**3**] Jia G, et al. J Magn Reson Imaging. 2011; 33(3):647-54, [**4**] Zhou J, et al. Prog. Nucl. Mag. Res. Sp. 2006; 48:109-36, [**5**] Henkelman MR, et al. Magn. Reson. Med. 1993; 29(6):759-66, [**6**] Henkelman MR, et al. NMR Biomed. 2001; 14(2):57-64.